Indian Journal of Chemical Technology
Vol. 29, January, 2022 pp. 9-22

Effects of operating variables in adsorption for azo textile dye from wastewater: Optimization of process parameters by Box-Behnken design of RSM: Isothermal and kinetic studies

H Upender*[,1], Srinivas Tadepalli[2] & Asif Afzal[3]

[1*]Department of Chemical Engineering, V.S.B. Engineering college, Karur 639111, Tamilnadu Indiaa

[2]Al Imam Islam University, Alfalah-Riyadh-Saudi Arabia -13314

[3]Department of Mechanical Engineering, P. A. College of Engineering, Mangaluru 574 153, India

E-mail: upender07053@gmail.com

Received 20 April 2021; accepted 10 November 2021

The removal of dye from azo textile dye using raw wheat bran adsorbent prepared by coating on low-density Polypropylene (PP) particles has been studied by batch experimental studies. The batch adsorption studies have been performed for 36 h. Box–Behnken design of response surface methodology (RSM) is utilized to ascertain the impact of initial concentration, adsorbent dose, and *p*H on the removal of dye. The data obtained from experimental parameters have been analyzed through the fitting of kinetic models such as Pseudo-first order, Pseudo second-order model, Intraparticle diffusion, and Elovich model for dye removal along with correlation or regression coefficient (R^2) values. The statistical analyses of the results collected in reaction kinetic modeling portray the superiority of the Pseudo second-order model for both dye removal. In the dye removal, the higher R^2 values are seen in case of better suitability of the Pseudo second-order model. The isotherms of adsorption experiments have been performed by employing different adsorption isotherm models such as Dubinin–Radushkevich, and Halsey. It is observed that both isotherms reflect the equilibrium data for dye removal.

Keywords: Azo textile dye, Batch study, Isotherm, Pseudo-first order model, Pseudo Second order model, Regression Coefficient, Wheat bran

The surface of Earth contains 70 % of water, which is the most precious natural resource on our planet. Life on Earth would not survive without this indispensable compound. Although this fact is commonly known, water resource contamination is a common problem that we are facing today. Strong contamination occurs directly through the discharge of waste from factories, refineries, and waste treatment plants, and indirectly via pollutants entering the water source through rainwater from soil/groundwater systems and the atmosphere. Industrial manufacturing is, to a large degree, responsible for environmental pollution. Lakes, streams, and seas are being polluted with numerous harmful impurities. On earth, water is the root of life. However, pollution is caused by different types of human activities, such as commercial, residential, and agricultural activities. For example, huge quantities of dyes are still present in wastewater from the material such as, sugarcane, oil refining, and textile industries[1]. The discharge of these pollutants is main reason for the irregular coloring of the surface waters. A few analysts discovered that material wastewaters are viewed as the most dirtied water on account of the presence of a high measure of colors that toxically affect the climate[2]. Chemical oxygen demand (COD), the containing of an enormous amount of total dissolved solids (TDS), suspended solids, salts, and natural accumulates[3,4]. Many of these innovations, however, are costly and complicated when used for the treatment of these dyes. As a result, the adsorption process tends to have the greatest prospect in the industry for wastewater cleaning[5], Thanks to its incredible ability to purify dirty water and economic factors[1]. A major contamination problem has been created by the finishing industry or textile dyeing as it is one of the effective chemically intensive industries on earth and the No. 1 polluter after agriculture for clean water[6]. There are large quantities of organic substances in textile dyestuffs that cause hindrance in the method of degradation and are aerobically difficult to discard. Organic compounds are observed to decline into carcinogenic agents under anaerobic conditions[7]. Interaction with textile dyes causes human issues including congenital

malformations, skin irritations, lung issues, sickness, and migraines[8]. An analysis has been established on the use of water hyacinth in reducing various pollutants in textile waste. The research is based on literature investigating the bio-sorption ability of hyacinth water in the removal of dyes, TSS (Total suspended solids), and COD (Chemical oxygen demand) concentrations in textile wastewater. The authors likewise have examined sorption energy through different models combination, the variables influencing bio-sorption concentration and the significance of physical and synthetic changes of water hyacinth for pollutants removal[9]. Moreover, much of the dye causes dangerous effects not only on human and animal wellbeing but also on microorganisms[10]. Therefore, for researchers, the elimination of dyes is the most important issue. Many new methods, such as biological therapy, have recently been adopted[11]. Any of the techniques for handling wastewater, including dyes, are physical and chemical procedures. Several studies have recently been done to produce adsorbents from different starting materials, such as waste materials[12-14], mango seed kernel[15], clay sawdust, and perlite[16-19] agricultural wastes[20], wheat bran was also used as removal of dye from industrial wastewaters[21]. Surface and *p*H have the major role to remove the methyl blue on wheat bran[22]. Ammonium salts-based modified wheat brans are used to remove the anionic dyes[23]. Different nonconventional adsorbents, including guar gum-based hydrogels, wheat bran, clay[24-26]. The key components of wheat bran contain hemi cellulose (29.2%), cellulose (32.1%), extractives (22.3%), and lignin (16.4%). Wheat bran can be used to extract toxic materials as an effective adsorbent. Due to various hydroxyl groups that exist in cellulose, hemicellulose, and lignin structures, wheat bran exhibits a low adsorption efficiency for anionic dyes. Practical and efficient surface modification of wheat brains to increase their an-ionic dye adsorption ability. To achieve a positive adsorbent, Yue et al. added amine groups to the structure of wheat bran by chemical modification[17]. Magnetic graphene oxide and Fe_3O_4 nanoparticles were loaded on the surface of wheat bran[27]. Dehydrated wheat bran is also the most effective adsorbent for the removal of methylene blue[28]. Different diameters of wheat bran particles have much removal efficiency for the Astrazon yellow 7G[29]. The tartaric acid-washed wheat bran is used as the most effective adsorbent for the removal of chromium from an aqueous solution[30,31].

While most of the researchers focused on the use of acid-treated wheat bran without airflow, only a few of the works[20-23,26] were reported on adsorption by treated wheat bran with some of the acids. In the present work, an attempt is made to identify the effect of parameters by the mechanism of adsorption of dye from an azo dye by natural adsorbent raw wheat bran. This wastewater treatment was achieved by coating the adsorbent on low-density polypropylene (PP) in batch adsorption processes. It was observed by changing the *p*H, initial dye concentration, and adsorbent load physicochemical characteristics of textile wastewater, characterization of adsorbent, dye removal efficiency, Isothermal, kinetic studies, and Box–Behnken design of (RSM) was also included.

Experimental Section

Adsorbent preparation

The natural material raw wheat bran was used in this investigation was obtained at Warangal, India, from a local flour mill. To avoid soluble impurities, the gathered wheat bran was cleaned off with DI water (De-ionized water). The wheat bran was washed and dried for 1-2 h in the oven at 70°C. Screening was done on the dried wheat bran. Upon screening for adsorbent preparation a fraction of 400 microns was obtained. Different grams of screened wheat bran fraction were taken in experiments for wastewater treatment. Weight the required amount of low density of Polypropylene (PP) solid particles and wheat bran on weighing balance. Now, add the binder to the PP Particles. Using a spatula/hand, coat the wheat bran on the PP particles properly and leave the adsorbent until it dries.

Stock solution preparation

The standard solution, which contains 1000 mg/L of textile dye was made by adding 0.5 g of textile dye powder in 1000 mL of distilled water. The spectrophotometer was used to measure absorbance.

Analysis of dye

An ultra-visible spectrophotometer (UV-1800 Shimadzu) was used for determining the dye intensity in samples at NIT, Warangal. In ultra-visible spectroscopy, a substance absorbs the light and it increases the energy of atoms present inside of that substance. This light may be visible light or ultra-visible light. It produces a spectrum.

Adsorption studies

The batch mode of processes was done in finding the removal rate and kinetic studies of dye. For

experiments, appropriate amounts of adsorbent were mixed with different concentrations of dye in the tapered inverse fluidized bed with assisted constant rate airflow rate from the bottom of the bed (Experimental setup shown in Fig. 1). The experimental setup is made up of acrylic glass with an inlet at the bottom and the outlet at the bottom for air, and it consists of an air compressor to supply the air, and control valves are used to control the air flowrate with a gas rotameter. The treated samples were collected at different time intervals from the bottom of the reactor. The effects of different parameters on the adsorption rate have been observed across different contact times and aeration was used to adsorption of dye removal increment on wheat bran. A noted amount of adsorbent was coated on low-density solids added in 3 L of the solution and noted concentrations apart, and then the solution was agitated in a tapered inverse fluidized bed with aeration.

The percentage of removal (R %) in a sample was determined using the equation (1)

$$R\ (\%) = \frac{C_0 - C_t}{C_0} \times 100 \quad \ldots (1)$$

where R is the % of dye removal.

C_0 = Dye initial concentration (mg/L) at time t=0

C_t = Dye concentration (mg/L) at time t.

Adsorption capacity measured using equation (2)

$$\%\ q_e = \frac{(C_0 - C_e)V}{W} \quad \ldots (2)$$

Where q_e is the adsorption capacity (mg/g)

Ce is the dye equilibrium concentration (mg/L), V is the solution volume (L), W is the adsorbent weight (g).

Different types of initial concentration of azo dye 100, 200, 350 and 450 mgL^{-1} and different amounts of the adsorbent dose were 1.5, 5.5 and 10 gL^{-1} were added to the initial concentration of dye solution. The effects on dye removal efficiency, isotherms, kinetics, and Box-Behnken design of RSM were investigated at various *p*H (1.6-8.9) values.

Results and Discussion

Characterization of adsorbent

Developed adsorbents were analyzed for their physical, chemical properties using different characterization techniques. The methodology for characterization and analysis is discussed as follows. Energy dispersive spectroscopy of prepared adsorbent was recorded by SEM-EDS system. The samples were laid down on metal grids and coated with platinum in a vacuum evaporator before analysis, Fourier Transform

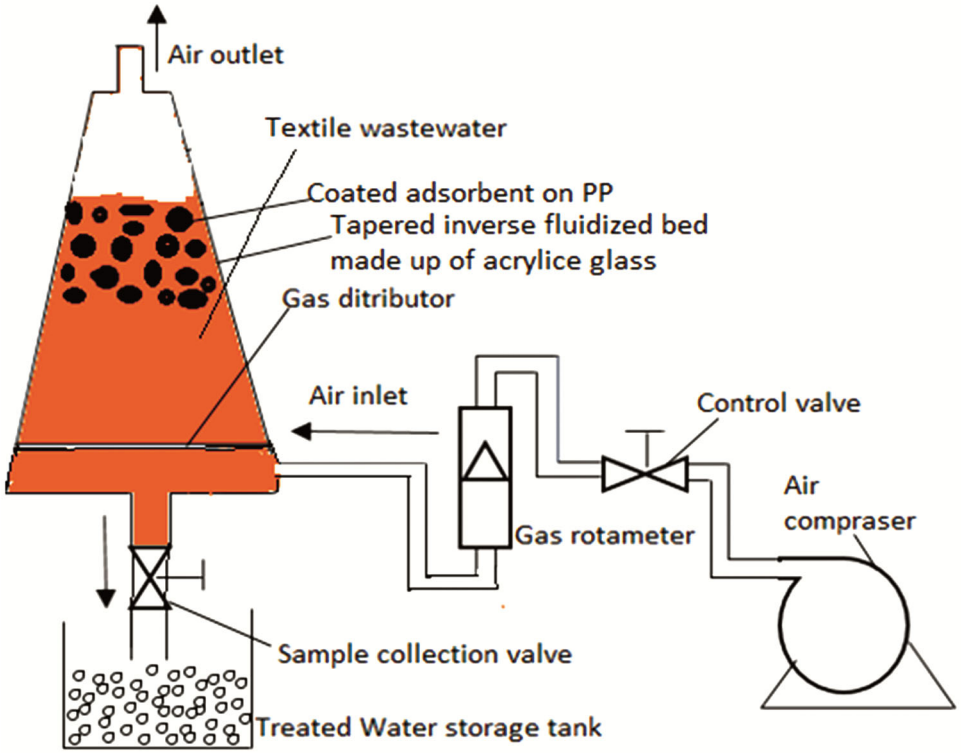

Fig. 1 — Schematic diagram of experimental setup

Infra-Red (FTIR) spectrophoto-meter (Perkin-Elmer, Model- FT-IR spectrum 2) was used for identification of functional groups present in prepared adsorbent at NIT, Warangal. FTIR spectroscopy was recorded by FTIR spectroscope (Perkin-Elmer).

SEM analysis combines with EDS

The Scanning electron micrograph (SEM) analyzer used for the examine the surface morphology from SEM micrographs the image confirms that the sample exhibits the form of the coarse surface but after coating on the PP the surface becomes porous and homogeneous shown in Fig. 2(a–d). Particle aggregation has been disrupted and particles are uniformly dispersed, creating a much surface area for adsorption. Further elementary measurement of raw wheat bran and coated wheat bran on PP was conducted with the help of EDS to measure its chemical distribution is observed in Fig. 3 (a, b). It was noted that they contain carbon and oxygen composition

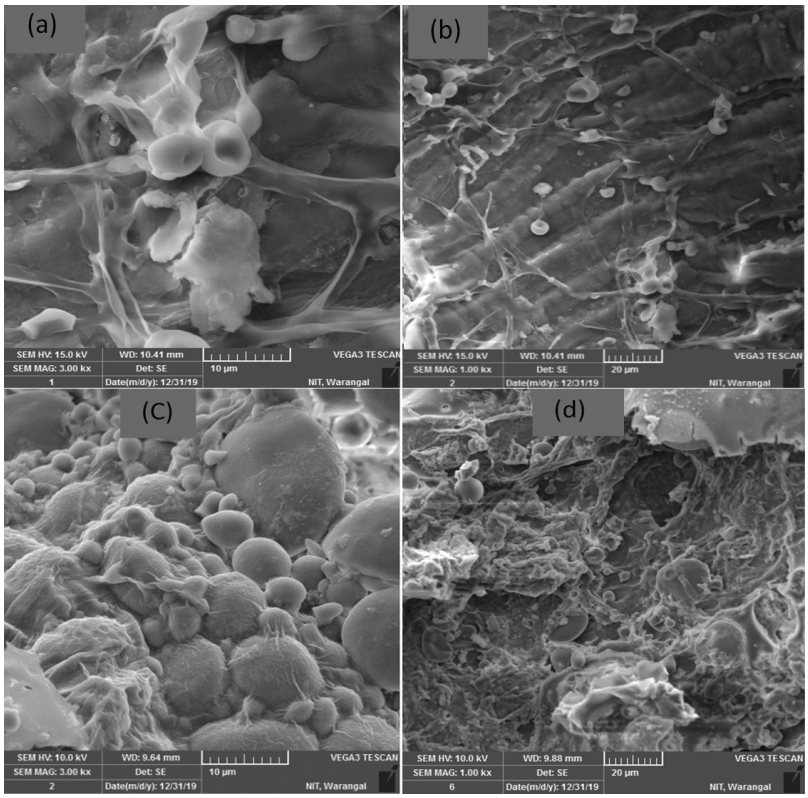

Fig. 2 — SEM of (a) Raw wheat bran at 10 µm resolutions, (b) Raw wheat bran at 20 µm resolutions, (c) Coated raw wheat bran on PP at 10 µm resolutions, and (d) Coated raw wheat bran on PP at 20 µm resolution.

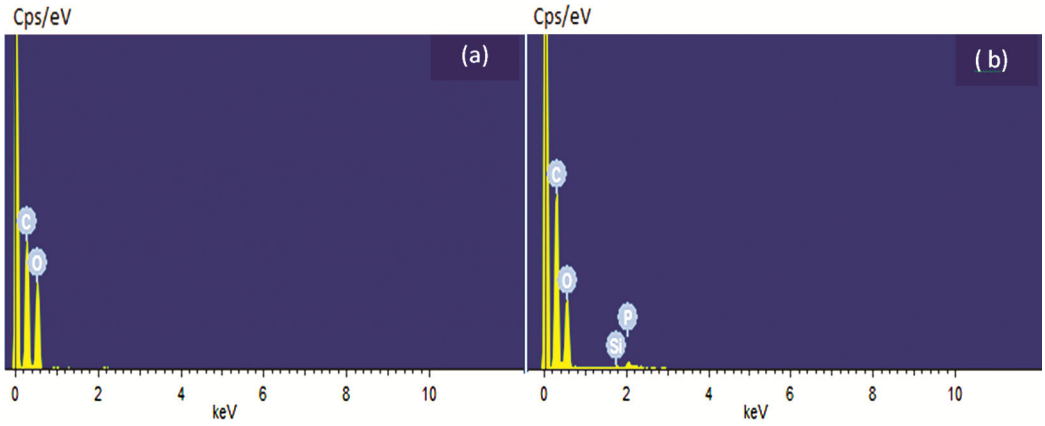

Fig. 3 — EDS spectra of the adsorbent (a) Raw wheat bran and (b) Raw wheat bran after coated on PP.

in cellulose was (49.40 and 50.60) wt percentage, respectively. However, after coating wheat bran on to PP, carbon wt% increases to 58.53 wt% oxygen decreases to 38.94 wt% (Table 1). Wheat bran, result in a raise of carbon composition (Table 1) and the improvement of active adsorption sites. This develops the behavior of wheat bran extraction.

Table 1 — Radical measurement of raw wheat bran and raw wheat bran coated on PP

Element	Raw wheat bran		Raw wheat bran ofter coating on Polypropylene	
	Weight %	Atomic %	Weight %	Atomic %
C	49.40	56.53	58.53	65.93
O	50.60	43.47	38.94	32.93
Si	x	x	0.66	0.32
P	x	x	1.87	0.82

FTIR

From the FTIR spectra of Figure. 4 (a, b), it was understood that both wheat bran and coated wheat

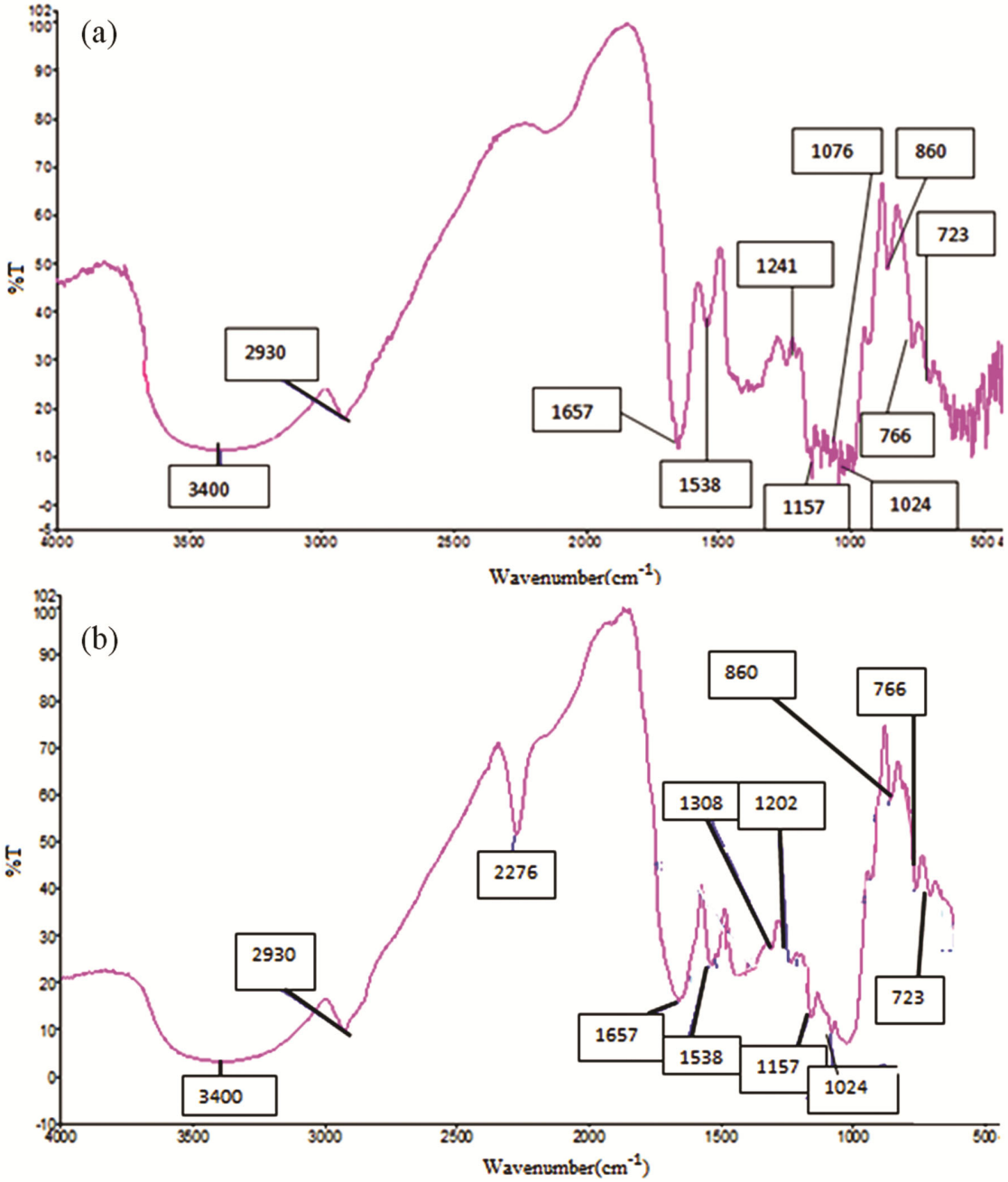

Fig. 4 — FTIR approach of (a) Raw wheat bran, and (b) Raw wheat bran after coated on PP

bran on PP had equal trends, but the intensity of the absorption bands was varied. In natural wheat bran, the peaks at 3400 cm^{-1} appeared stretching vibrations, suggesting the existence of cellulose. From the FTIR spectra of Fig. 4 (a, b), it was understood that both wheat bran and coated wheat bran on PP had equal trends; however, the intensity of the absorption bands was varied. Similarly, the carboxyl group adsorption band at 1538 cm^{-1} was killed by coated wheat bran on PP. The peaks at 1157, 1241, 1024, and 1076 cm^{-1} indicate the existence of the C-O-C group in natural wheat bran. Also, peaks at 860, 766, and 723 cm^{-1} have vanished in coated wheat bran on PP. There is a peak of 1657 cm^{-1} in the raw wheat bran due to the C = O group. The peaks are 1202 cm^{-1} and 1308 cm^{-1}, showing C -C and C-O groups in the coated wheat bran on PP.

Effect of *p*H

The effect of *p*H on removal of dye on raw wheat bran was studied. It was seen that when the initial *p*H of the solutions increased the removal percentages of dye were also be varied. The variance of the removal rate and adsorption capacities of azo dye on wheat bran at different *p*H values was studied. The alkaline state was favourable for the adsorption of dye on wheat bran, when the initial dye concentration was 100, 200, 350, and 450 mg·L-1, the adsorption capacities are 42.58, 254.23,559, and 767 mgL-1at natural *p*H value of 3.3, and the adsorption capacities of azo dye were 48.1, 252.3, 560.84 and 771.38 mg/g at a *p*H of 8.5. Thus, the rate of adsorption and capability of adsorption are decreased with *p*H Value. Consequently, the adsorption capacities and adsorption rate are decreased with *p*H value. The *p*H of the dye samples dominance the extent of ionization of the acidic and basic nature of the dye and the effecting nature of the surface of the adsorbent[32].

It was observed that with a hike in *p*H to 1.6, the degradation of dye had been raised slowly, whereas dye removal and the solidification rate of organic carbon have been diminished after *p*H 2.5. From the getting data, it has been seen that *p*H 2.5 is an ideal value to determine desired value. This was because of the adsorption of azo dye on the adsorbent outer surface which is dependent on its surface activated. At pH 2.5, the wheat bran surface may be negatively activated because of the creating of enormous hydroxyl groups, which works on the adsorption of azo dye and being-sharpened collapse[33].

Additionally, the sample *p*H > 2.5 might have to grant negatively activated to the adsorbent surface, accordingly obstruct dye removal by reducing dye ions adsorption on the adsorbent surface. It was presented that the generation of hydroxyl radical was supported at low *p*H. Be that as it may, the hydroxyl ions can also be created by prowling the photo-generated openings on the outside of the adsorbent. These hydroxyl ions rival the optimization model collapse of dye caused by holes in the wheat bran depletion region. Amin[37] was found that the adsorption of reactive dyes on activated carbon which was made from sugarcane bagasse which outcome achieved that the dye adsorption was optimum at initial *p*H of 2.5 and rise in *p*H diminishes the (%) of dye removal. Given the literature survey, the addition of evacuation for cationic dye at high *p*H because of the reduction of positive activation at the solution interfaces which coming about the adsorbent surface to be negatively activated. As the improvement of dye adsorption at low *p*H value as a consequence of adsorbent surface seem, by all accounts, to be decidedly charged because of positive charge increase in solution interface.

Effect of Adsorbent Dose

The impact of the adsorbent dose on the dismissal of dye was analyzed by varying the adsorbent dose in the adsorption method. In the different experiments, the bed was filled with 3 L of azo dye synthetically prepared water having varies 100,200,350 and 450 mg/L of concentrations for dye removal studies. All the experiments were done at the same adsorbent doses are 1.5, 5.5, and 10 g/L.

The process temperature of the adsorption processes was kept constant at room temperature. From the outcomes, it was found that the 5.6 g/L of adsorbent dose gives the maximum adsorbent activity towards the removal of azo dye in an aqueous solution. About 89% of the dye was obtained by an adsorption mechanism. The impact of the dosage of the adsorbent for dye removal, the percentage diminish of dye was studied.

From the observed results, it was found that above 5.5 g/L of adsorbent dosage has indicated lower dye removal. This effect may be attributed to the accumulation of adsorbate molecules during excessive loading, implying that dye molecule adsorption was reduced due to the limited availability of the catalyst surface's total available active sites. Also, higher adsorbent loading has resulted in high wastewater

turbidity, which during adsorption processes minimizes the adsorption nature of wastewater on the adsorbent surface. Ultimately, smashing with ground-state molecules deactivates the active adsorbent particles. This study concludes that the dose of 5.5 g/L adsorbents is adequate to achieve good azo dye decolorization using the adsorption method. Therefore, as an ideal adsorbent dosage for azo dye removal, 5.5 g/L of wheat bran adsorbent was observed and further experiments were done with this optimized adsorbent dosage.

Effect of initial dye concentration

The effect of increasing the initial concentration of dye would increase the ability of adsorbent loading[35]. The removal of azo dye in the adsorption method was investigated by varying initial dye concentrations were 100,200,350 and 450 mg/L respectively and the adsorbent dose was kept constant as 5.5g/L. The treated samples were gathered at periodic time intervals from the bottom of the reactor and were measured by UV absorbance to analyze the removal of a percentage of dye. From the experiments, it was found that an increase in the dye, lead to less removal.

A given amount of sorbent can just adsorb a specified quantity of dye, consequently, the initial dye concentration of a sample is one of the significant parameters to examine[36]. Figure 5 (a, b) which is given in supplementary data explains the impact of initial concentration on the effectiveness of adsorption processes. The reduction in the removal of dye at higher initial concentrations is because of less reactivity of hydroxyl radicals. The other reason may be the low adsorption of dye on the surface of the adsorbent. It was identified that the proficiency of the cycle was improved at significantly higher initial concentrations concerning the total measure of dye removal. The initial dye concentrations to use in this task are 100, 200, 350, and 450 mg/L these concentrations have indicated removal of about 93.5, 83.54, and 79.24 for dye respectively.

From the present obtained results, it was observed that the removal of dye diminishes with the hike of dye concentration. The consistent contact time and adsorbent surface are the reasoning for this hike. Because of the surface given by the adsorbent, the dye has been adsorbed on its surface. From the literature work, it is noticed that the close connection between the accessible surface site on adsorbents and the concentration of dye influence the initial concentration variables[37]. As the initial concentration increment, the access site on the adsorbent surface region becomes less which causing an addition in dye been adsorbed.Although, the rejection of dye rate diminished[38].

Model development, Regression analysis and optimization through RSM

In the course of recent many years, various analysts have focused their endeavors on optimizing wastewater treatment systems utilizing various models. The RSM technique has been demonstrated to be a productive improvement model for working factors. To enhance the operating boundaries like flocculent, *p*H, and coagulant dose for the treatment of paper reusing wastewater, the reaction surface technique (RSM) was presented[39]. The experiments of confirmation have revealed the RSM is the most effective approach for optimizing initial coagulation-flocculation process parameters[43].Studies of the impact of process variables on the testing of refinery wastewater in submerged

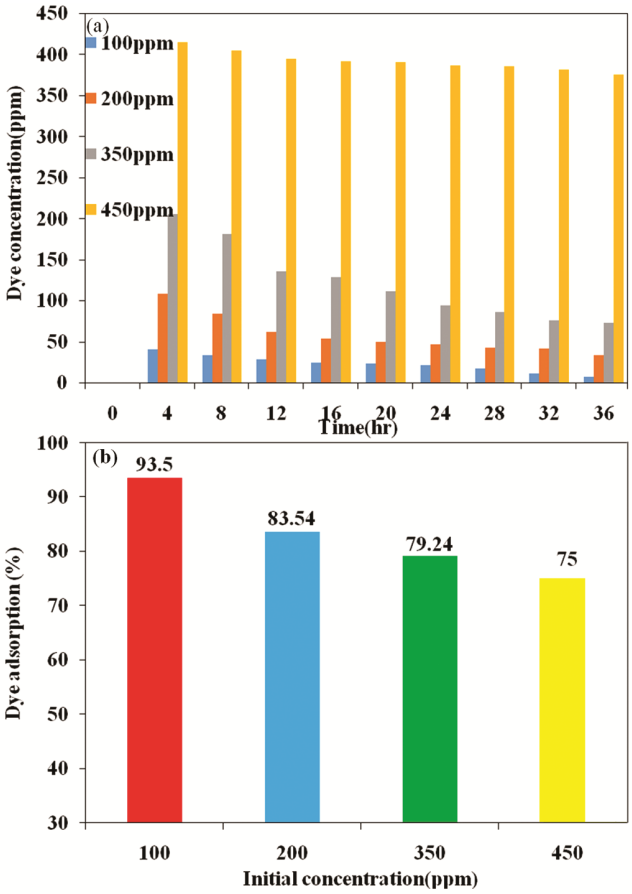

Fig. 5 — (a) Effect of initial dye concentration in the adsorption processes [adsorbent dose = 5.5 g/L, *p*H = 1.6]; (b) Effect of initial dye concentration on % of dye removal in adsorption processes [Initial *p*H = 1.6, adsorbent dose = 5.5 g/L].

ultrafiltration. In this investigation, different variables those are *p*H, hydraulic retention time (HRT), and mixed liquor suspended solids (MLSS) concentration were optimized by utilizing response surface methodology (RSM). From the acquired outcomes it was found that the benefit of RSM had outperformed the evacuation of water flux and COD[44].

In the present work, three operating variables shown in Table 2 were used to design Box-Behnken matrices for both dye removal. A good model fit is needed to optimize the response surface. An appropriate model is required to avoid poor outcomes. Figures 6 display actual and predicted adsorption graphs for dye elimination. From Fig. 6 which is shown in supplementary data, the actual R^2 value and adjusted R^2 value were observed to be 0.915 for dye. Furthermore, the R^2 value specifies the model's goodness of fit. In our work, the R^2 value indicates that regression models are well-suited to achieving the desired outcomes.

The second-order quadratic mathematical model Eqn (3) was derived from experimental results and analyses the difference within dye removal quality, and control variables (A, B, C). The final equation for both in terms of Coded factors:

$$\% \text{ Azo dye removal}=78.64-5.90A-2.95B+9.26C +2.32AB+0.6725-0.5325B0.8572A^2+3.67B2 +2.99C^{2.} \quad \ldots (3)$$

In this case, the experimental and expected findings are more likely to be accurate. The R^2 value was used to observe the precision of the predicted results and to observe the correlative performance of the experimental results. The obtained equations 3 have been used to compare the experimental and predicted findings. From experimental and predicted observations, it was indicated that the correlation coefficient was good (R^2=0.98), and from the experimental results, it was found that the correlation coefficient was also effective (R^2=0.985). The Modified R-squares for these theories were closer to the R-squared value and had a higher coincident value.

The ANOVA for the Response surface model was conducted and the findings were given in Table 3. The findings from the experiment were agreed as being accurate, valid, and predictable. In the ANOVA analysis, the model variance and the residual variance can be compared using the F-test. When the fit is not very less, it will be noted if Prob>F-value. Demonstrating A, B and C are efficient models. The R^2 esteems in this investigation were best a result of the best fit of the model[45]. Not only R^2, but the fitness

Table 2 — Box-Benkhan operating factors and their levels

Factor coded values	Levels		Response
	Low	High	
pH	1.6	8.9	Dye removal
Initial concentration(mg/L)	100	450	
Adsorbent dose(g/L)	1.5	10	
Air flowing time(hr)	4	36	

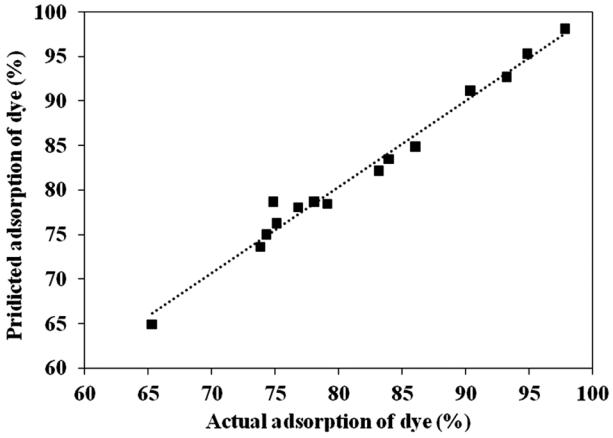

Fig. 6 — Actual and predicted removal (%) graphs for dye.

Table 3 — ANOVA analysis of variance table for dye removal

Source	Sum of Squares	df	Mean Square	F-value	p-value	
Model	1158.40	9	128.71	17.48	<0.0001	significant
A-Concentration	278.24	1	278.24	37.78	0.0005	
B-pH	69.50	1	69.50	9.44	0.0180	
C-Adsorbent dose	685.61	1	685.61	93.09	< 0.0001	
AB	21.58	1	21.58	2.93	0.1307	
AC	1.81	1	1.81	0.2456	0.6353	
BC	1.13	1	1.13	0.1540	0.7064	
A^2	3.09	1	3.09	0.4201	0.5375	
B^2	56.80	1	56.80	7.71	0.0274	
C^2	37.59	1	37.59	5.10	0.0584	
Residual	51.55	7	7.36			
Lack of Fit	7.65	3	2.55	0.2323	0.8699	not significant
Pure Error	43.90	4	10.98			
Core total	1209.96	16				

of the obtained model equations was also justified by utilizing residuals. The normality of the residuals can be measured by using normal probability graphs. The residuals represented in Fig. 7(a) were indicated against the anticipated data. Better outcomes can be indicated in Fig. 7(b).

The objective of the current task is to find the optimized input process variable data for the removal of dye from the wastewater treatment by utilizing the adsorption method. Experimental design equations were used to minimize the input process variables. The feasible data of the process variables for the ultimate output of the dye removal efficiencies were observed to be 5.5g/L, 2.514, and 99.55 ppm for Adsorbent dose, *p*H, and initial concentration, respectively. At such optimized points, the predicted and experimental results were noted azo dye removal (%) were 88.06, 89.50, respectively. Figure 8 represents the response surface, contour graphs and designed for the optimization of processes variables for dye removal utilizing the system. The maximum removal was obtained when the experiments were carried out at the achieved optimum data. By using the optimized operating variables built in the RSM, this can be inferred as the best method for efficient elimination. Hence this study is termed as better fitted.

Adsorption isotherms

In recent times, the sorption isotherm depicts how adsorbed species come into contact with adsorbent materials and hence is essential in optimizing the use of adsorbents. Equilibrium isotherm is explained as a sorption isotherm, described by some of these coefficients whose data values represent the surface characteristics and ability of the sorption equilibrium because when the concentration of sorbate in the bulk solution is dynamically balanced with that of the sorbent interface[41]. The fitting of equilibrium adsorption data to various isothermal analyses is a critical step to determine an effective model for design purposes[42]. The adsorption isotherm is essential for the explanation of how much the adsorbate comes into contact with the adsorbent and provides an estimate of the adsorption capacity of the adsorbent. The surface phase can be assumed as monolayer or multilayer[43]. In optimizing the design of the dye removal adsorption system, it is significant to develop the much more acceptable equilibrium data correlations between each model. The values were determined from the correlation seen between the quantity of contaminant focused on the surface of the adsorbent and that remaining in the bulk solution at a given temperature may indicate the ability to bind the adsorbent to the adsorbent. Two isothermal models were evaluated in the current Dubinin–Radushkevich and Halsey models. The implementation of isothermal equations is contrasted by assessing the coefficient of correlation, R^2.

Dubinin–Radushkevich model

The assumption in the D–R isotherm model eqn (4) is not dependent on a homogeneous surface; it provides data on biomass permeability and adsorption energy.

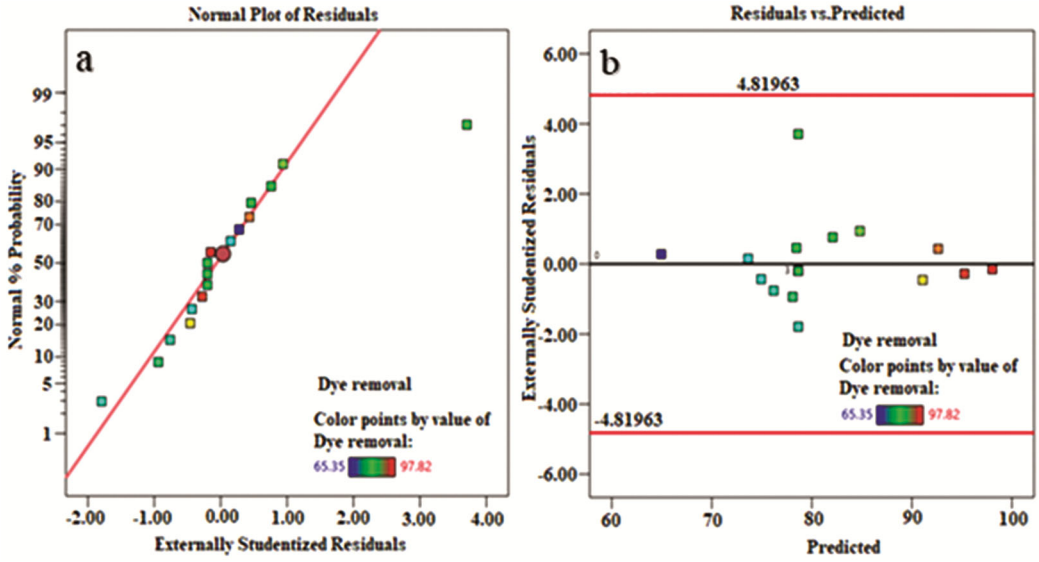

Fig. 7 — (a) Normal graphs of Residuals, (b) Residuals vs Predicted for dye removal

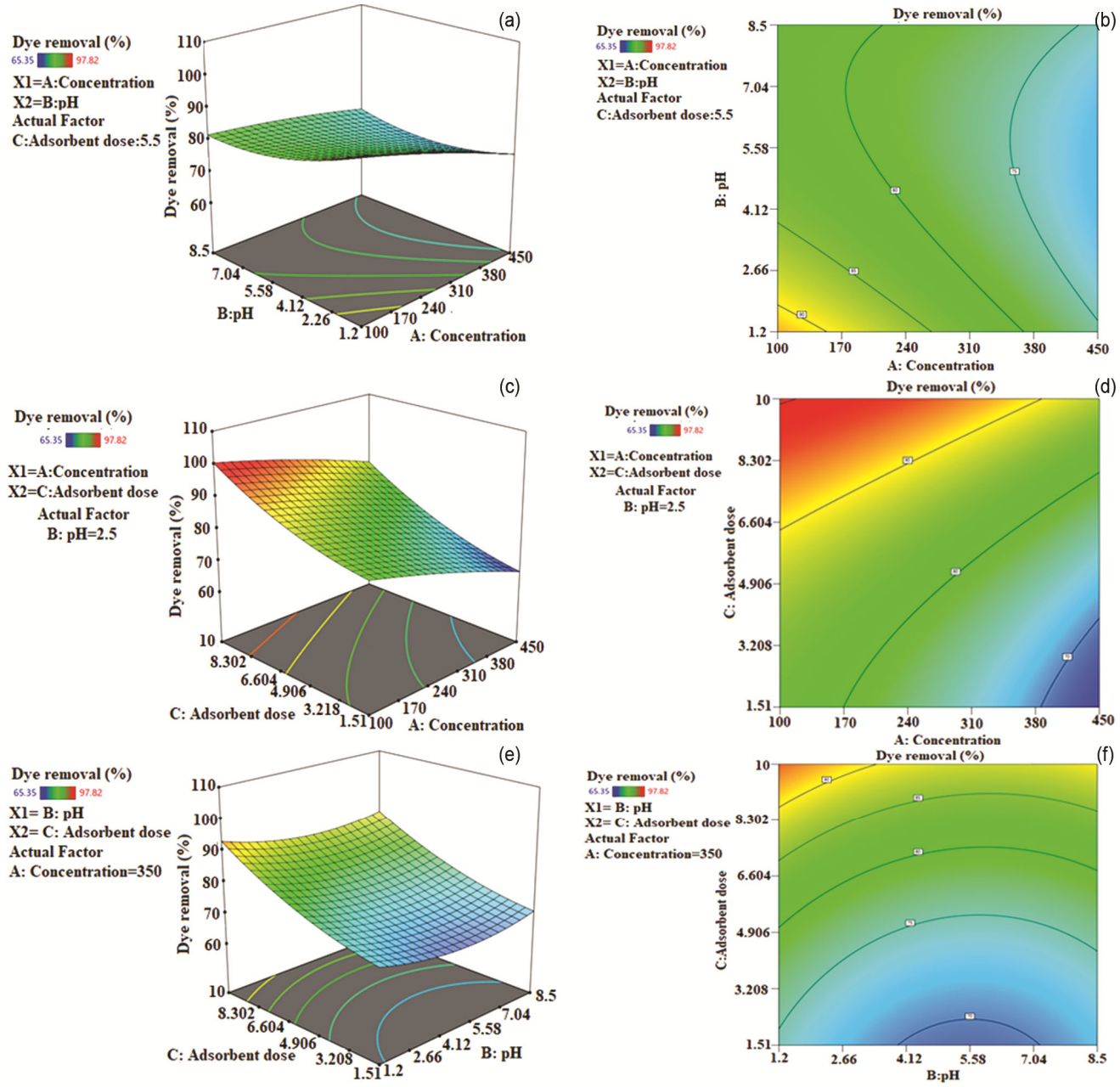

Fig. 8 — Response surface graph indicated process associates with the input variables to increase % dye removal. (a) *p*H Vs concentration; (c) Adsorbent dose Vs concentration; (e) Adsorbent dose vs *p*H and 10 (b, d, f) are contour graphs.

$$lnq_e = lnq_m - \beta\mathcal{E}^2 \quad \ldots (4)$$

Where $\mathcal{E} = RTln[1 + \frac{1}{C_e}]$, $E = [\frac{1}{SQRT(2\beta)}]$

Halsey model

The Halsey (Halsey, 1948) adsorption isotherm can be shown below:

$$lnq_e = \frac{1}{n}[lnK_H - lnC_e] \quad \ldots (5)$$

The Halsey isotherm constant and exponent are K_H and n, respectively. The equation (5) is perfect for multilayer adsorption, and the experimental evidence fitting this equation attests to the adsorbent's heterogonous existence. The adsorption energy value also indicates whether the adsorption mechanism is chemical or physical. The equilibrium values for fitting D–R and Halsey isotherm models for dye removal was calculated. Table 4 shows the data of the

isotherm parameters, and R^2 root means square error. The D–R and Halsey isotherms are found to be the most appropriate for dye removal.

Table 4.Isotherm constants for adsorption of dye on raw wheat bran at optimum conditions.

Adsorption kinetics

The investigation of adsorption kinetics explains the solvent uptake rate and obviously, this rate regulates the residence time of adsorbate uptake at the solid sample interface. The kinetics of the dye removal on adsorbent was studied utilizing pseudo-first-order and pseudo-second-order[44].

Pseudo-first order equation

The rate of adsorption is directly proportional to the number of vacant sites when considering reversible binding contaminants and adsorption on active sites present on the adsorbent surface. The equation of pseudo-first-order was expressed by Eqn. 6

$$\frac{dq}{dt} = k_1 (q_e - q_t) \quad ...(6)$$

Where q_t and q_e are the adsorption capacity at time t and equilibrium, respectively (mg/g).k_1 is the rate constant (min^{-1}). Integrating and implementing the above equation boundary conditions from t = 0 to t = t, and q_t = 0 to q_t = q_t, the integrated form of Eqn.7becomes

$$\log (q_e - q_t) = \log (q_e) - \frac{k_1 t}{2.303} \quad ...(7)$$

Eqn. 7applies to the experimental results. The rate constant in this model was investigated by the slope of the graph of ln (Qe − Qt) over time (t).

Pseudo second order equation

In this model, it was considered that capability of adsorption of adsorbate on the adsorbent surface is affected by chemical forces, instead of physical attrition forces.

Non-linear form of the model is given as

$$\frac{dq}{dt} = k_2 (q_e - q_t)^2 \quad ...(8)$$

Upon integration with boundary conditions from q_t = 0 at t = 0, q = q_t at t = t, the above equation (Eqn.8) Reduces to desired eqn (9)

$$\frac{t}{q_t} = \frac{1}{k_2 q_e^2} + \frac{t}{q_e} \quad ... (9)$$

Where q_t and q_e are the adsorption capacities time t, and at equilibrium respectively (mg/L). k_2 is the rate constant (g/mg.min).The rate constant was investigated for different dye concentrations according to the graph of t/q_t versus t, as indicated in Figure 9 which is given in supplementary data. The determined (R^2) were observed to be greater than 0.98, and the determined Qe varied from the experimental ones are shown in Table 5 which is given in supplementary data. Depending on the results of the pseudo-second-order kinetic model, Qe, cal had better coincidence with the experimental Qe, exp shown in Fig. 10 which is given in supplementary data at different adsorbent doses and *p*H is1.6. This characterization shown in the pseudo-second-order model was a good model to illustrate the adsorption method of azo dye removal on wheat bran.

Table 4 — Isotherm constants for adsorption of dye on raw wheat bran at optimum conditions.

	D-R Model			Halsey model		
	β	q_m	R^2	K_H	n	R^2
Dye	0.0082	174.16	0.974	8.11	2.79	0.949

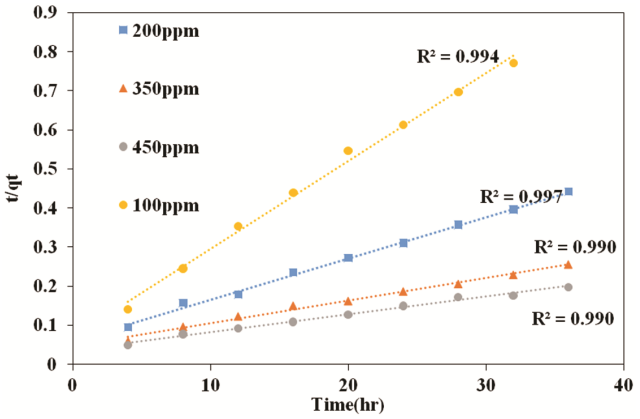

Fig. 9 — Pseudo-second order graph for dye removal for the adsorption of azo dye on wheat bran at varies initial concentration, pH=8.5, adsorbent dose=5.5g L^{-1}

Table 5— Pseudo-First-Order model and Pseudo-Second-order model for removal of azo dye by Wheat bran.

C_O(ppm)	Q_{exp}	Pseudo first order			Pseudo second order		
		K_1	Q_{cal}	R^2	K_2	Q_{cal}	R^2
100	45.58	0.00561	19.95	0.97	0.00719	44.04	0.99
200	82.22	0.095	84.52	0.97	0.0018	94.33	0.99
350	140.47	0.15	199.5	0.99	7.15*10^-5	172.41	0.99
450	182.39	0.063	131	0.97	5.93*10^-4	215	0.99

Intraparticle diffusion model

In the way of determining the mechanism of the azo dye adsorption on the raw wheat bran which was coated on PP, intra-particle diffusion depends on the process is investigated. The best common method for finding the process incorporated in the adsorption method is, suiting an intra-particle diffusion graph. As per the theory suggested by Weber and Morris[45], it is an experimentally determined functional connectivity, most adsorption-related method, where uptake changes nearly relatively with $t^{0.5}$ instead of with contact time. Eqn (10) is shown below.

$$.q_t = K_{ip} + C_i \quad \ldots (10)$$

Where kip= Rate constant of the intra-particle diffusion model ($mg \cdot g^{-1} \cdot min^{-1/2}$),

Ci = Constant related to boundary layer thickness (mg·g−1), both constants can be measured from intercept and slope of the graph of q_t versus time $t^{0.5}$. As the straight line that does not passes via the origin by the inter-particle diffusion model, state that the substance adsorption mechanism was not only regulated to the intra-particle diffusion but also effect by other methods. The model graphs were shown in Fig. 11 which is given in the supplementary file. The constants Kip and C_i were observed to grow with an increment of dye concentration, which could be because of the increment of the boundary layer thickness (as indicated in Table 6 which is given in supplementary data). These high results showed that the external diffusion of azo dye atoms on wheat bran was useful in the initial adsorption era. Higher values of R^2 closer to 1 suggest a greater preference for the intra-particle model of adsorption.

The Elovich model

The Elovich process model of adsorption is described as an equation (11) that became a choice of the process that explains adsorption in a non-ideal state of matter. Two types of adsorption can be summarized as immediate adsorption and moderate adsorption.

$$q_t = \frac{1}{\beta} ln\alpha\beta + \frac{1}{\beta} lnt \quad \ldots(11)$$

Where α is the initial rate of adsorption (mg·g−1·min−1) and β is the coefficient of desorption ($mg \cdot g^{-1}$). The plot of qt versus ln t is a line with an intercept of 1/β ln (α β) and a slope of 1/β. The correlation coefficient (R^2) at azo dye concentrations of 100, 200,350, and 450 $mg \cdot L^{-1}$ at a different adsorbent dose and *p*H values were given. The model plots were shown in Fig. 12, which are given in supplementary data. The fitting values determined from Elovich kinetic model observed that when the initial concentration of azo dye concentration was 100 $mg \cdot L^{-1}$ at an adsorbent dose of 5.5 g and *p*H 2.5,

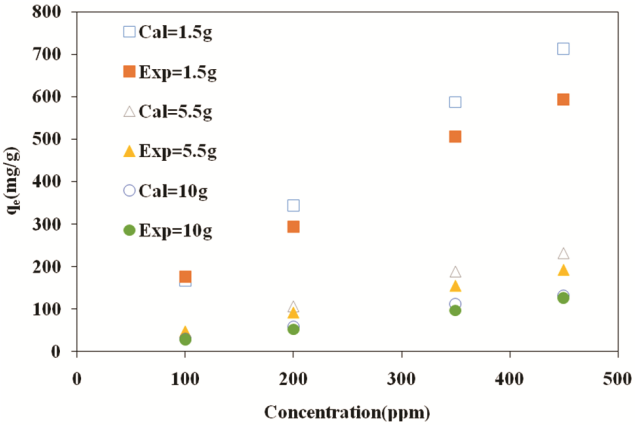

Fig. 10 —Pseudo-second order graph for adsorption capacity with experimental data for dye on wheat bran at varies initial concentrations at *p*H=1.6

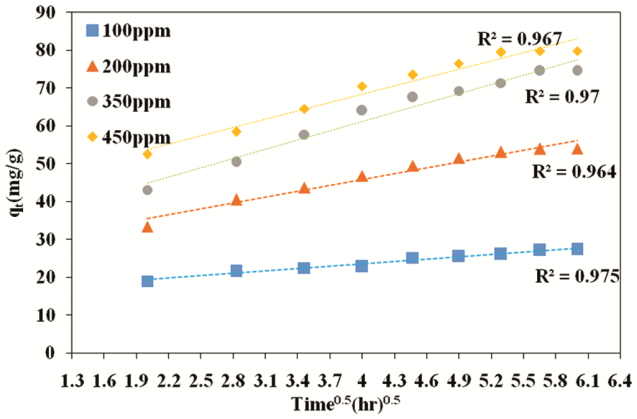

Fig. 11 —Intraparticle diffusion plot for adsorption of azo dye on wheat bran for varies initial dye concentrations on Wheat bran for varies initial dye concentrations.

Table 6 — Intraparticle diffusion and Elovich model for removal azo dye by Wheat bran

C_O(ppm)	Intraparticle diffusion			Elovich model		
	K_{ip}	Ci	R^2	α	β	R^2
100	3.86	23.2	0.96	102.92	0.141	0.922
200	10.77	24.606	0.97	41.8	0.052	0.93
350	20.112	33.08	0.97	54	0.027	0.962
450	24.14	28	0.98	51.935	0.022	0.956

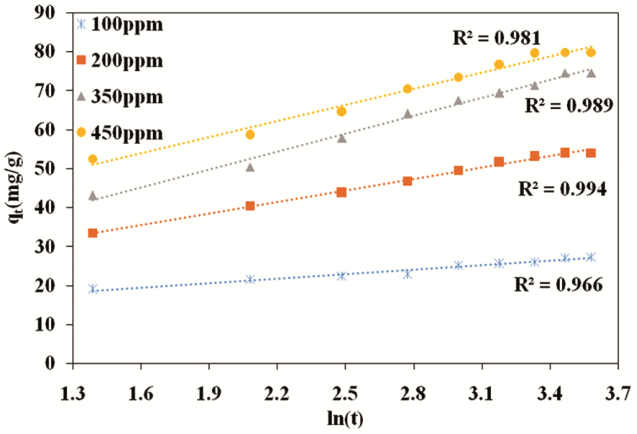

Fig. 12 —Elovich model plot for adsorption of azo dye on wheat bran for varies initial dye concentrations on wheat bran for varies initial dye concentrations

the model find that the obtained results not good. However, based on the experiments that can be well defined by the Elovich model, it can be viewed that the initial concentration of azo dye concentration was higher than 100 $g \cdot L^{-1}$ implying that the rate-limiting step was the Intraparticle diffusion method and not just the method[34].

Conclusion

The outcome in this work show that raw wheat bran is a successful adsorbent for the removal of azo dye removal. From obtained outcomes in the present work, it has been found that the adsorption treatment with wheat bran adsorbent is efficient. At adsorbent loading of 5.5g/L, Initial dye concentration 99.55mg/L, and *p*H 2.5, these are accounted as optimum process variables for dye removal respectably. The removal efficiency of dye by raw wheat bran reached 88.06 % and it is observed that on enhancing *p*H and initial concentration of the dye sample, the removal of dye is diminished. It could be assumed that the good approach for essential dye removal utilizing optimum process variables designed in the RSM experimental model. The equilibrium data fitted well to both D-R and Halsey isotherms, the adsorption is confirmed with the pseudo-second-order model from kinetic studies and also adopted with the intra-particle diffusion and Elovich models. The overall rate of dye uptake is observed to be controlled at starting of the adsorption, while interparticle diffusion regulated the total rate of adsorption at a later stage.

Conflict of interest

The authors declare that there is no conflict of interest

References

1 Peker S, Yapar S & Beşün N, *Colloids Surf A: Physicochem Eng Asp*, 104 (1995) 249.
2 Lourenco N D, Novais J M & Pinheiro H M, *Water Sci Technol*, 42 (2000) 321.
3 Liu S, *Chem Eng J*, 248 (2014) 135.
4 Yao Z Y, Qi J H & Wang L H, *J Hazard Mater*, 174 (2010) 137.
5 Ncibi M C, Mahjoub B & Seffen M, *Int J Environ Sci Technol*, 4 (2007) 433.
6 Kant R, *Nat Science*, 04 (2012) 22.
7 Jain R, Bhargava M & Sharma N, *Indust Eng Chem Res*, 42 (2003) 243.
8 Allègre C, Moulin P, Maisseu M & Charbit F, *J Mem Sci*, 269 (2006) 15.
9 Sanmuga Priya E & Senthamil Selvan P,*Arab J Chem*, 10 (2017) S3548.
10 Lemlikchi W, Drouiche N, Belaicha N, Oubagha N, Baaziz B & Mecherri M O, *J Indust Eng Chem*, 32 (2015) 233.
11 Naresh B, Jaydip J, Prabhat B & Rajkumar P, *Int Res J Biol Sci*, 2 (2013) 77.
12 Weng C H & Pan Y F, *Colloids Surf A: Physicochem Eng Asp*, 274 (2006) 154.
13 Kumar K V, Ramamurthi V & Sivanesan S, *J Colloid Interf Sci*, 284 (2005) 14.
14 Rozada F, Calvo L F, García A I, Martín-Villacorta J & Otero M, *Bioresour Technol*, 87 (2003) 221.
15 Kumar K V & Kumaran A, *Biochem Eng J*,27 (2005) 83.
16 Acemioğlu B, *Chem Eng J*, 106 (2005) 73.
17 Gürses A, Doğar Ç, Yalçin M, Açikyildiz M, Bayrak R & Karaca S, *J Hazard Mater*, 131 (2006) 217.
18 Doğan M, Alkan M, Türkyilmaz A & Özdemir Y, *J Hazard Mater*, 109 (2004) 141.
19 Garg V K, Amita M, Kumar R & Gupta R, *Dyes Pigments*, 63 (2004) 243.
20 Kannan N & Sundaram M M, *Dyes Pigments*, 51 (2001) 25.
21 Das S, Singh S & Garg S, *Orient J Chem*, 35 (2019) 1565.
22 Alzaydien A S, *Orient J Chem*, 31 (2015) 643.
23 Zhang W X, Lai L, Mei P, Li Y, Li Y H & Liu Y, *Chem Phys Lett*, 710 (2018) 193.
24 Zhong Q Q, Yue Q Y, Li Q, Xu X & Gao B Y, *Desalination*, 267 (2011) 193.
25 Thombare N, Jha U, Mishra S & Siddiqui M Z, *Carbohydr Polym*, 168 (2017) 274
26 Ong S T, Lee C K &Zainal Z, *Bioresour Technol*, 98 (2007) 2792.
27 Ge H, Wang C, Liu S & Huang Z, *Bioresour Technol*, 221 (2016) 419.
28 Özer A & Dursun G, *J Hazard Mater*, 146 (2007) 262.
29 Sulak M T, Demirbas E & Kobya M, *Bioresour Technol*, 98 (2007) 2590.
30 Kaya K, Pehlivan E, Schmidt C & Bahadir M, *Food Chem*, 158 (2014) 112.
31 Singh K K, Hasan S H, Talat M, Singh V K&Gangwar S K, *Chem Eng J*, 151 (2009) 113.

32 Fu J, *Chem Eng J*,259 (2015) 53.

33 Lu C, *J Mol Catal A: Chem*, 310 (2009) 159.

34 Amin N K, *Desalination*,223 (2008) 152.

35 Adeyemo A A, Adeoye I O & Bello O S, *Appl Water Sci*, 7 (2017) 543.

36 Bharathi K S & Ramesh S T, *Appl Water Sci*, 3 (2013) 773.

37 Ould Brahim I, Belmedani M, Belgacem A, Hadoun H & Sadaoui Z, *Chem Eng Transact*, 38 (2014) 121.

38 Azhar S S, Liew A G, Suhardy D, Hafiz K F & Hatim M I, *Am J Appl Sci*, 2 (2005) 1499.

39 Khannous L, Abid D, Gharsallah N, Kechaou N & Boudhrioua Mihoubi N, *Afr J Biotechnol*, 10 (2011) 13823.

40 Mokhtar N M, Lau W J, Ismail A F, Youravong W, Khongnakorn W & Lertwittayanon K, *RSC Adv*, 5 (2015) 38011.

41 Oladoja N A, Aboluwoye C O & Oladimeji Y B, *Turkish J Eng Environ Sci*, 32 (2008) 303.

42 Haghseresht F & Lu G Q," *Energy Fuels*, 12 (1998) 1100.

43 Salleh M A M, Mahmoud DK, Karim W A W A & Idris A, *Desalination*, 280 (2011) 1.

44 Hamadi N K, Chen X D, Farid M M & Lu M G Q, *Chem Eng J*, 84 (2001) 95.

45 Hameed B H, *J Hazard Mater*, 162 (2009) 344.